A White-Box Quantification Framework for Hidden Thermal Losses in 110kV Oil-Immersed Power Transformers Based on Green-Zone Dual Stress

Yi Zeng

Abstract—In modern grids, the synergistic effect of sub-threshold harmonics (THD $\leq$ 5%) and periodic minor overloads (load factor $K \leq 105\%$) accelerates the thermal fatigue of 110kV oil-immersed transformers. Since these stresses remain within standard compliance boundaries (IEEE Std 519 and IEC 60076-7), they evade static SCADA alarms, creating a critical monitoring blind spot. To address this, this paper formally defines this operational state as the Green-Zone Dual Stress (GZDS) scenario. We propose a white-box dual-engine physics-informed framework tailored for GZDS, integrating the IEEE Std C57.110 eddy current loss factor and the IEEE Std C57.91 Arrhenius thermal aging equation to precisely quantify hidden lifespan losses. Anchored on the standard 20.55-year baseline design life, one million Monte Carlo evolutionary simulations reveal that GZDS synergy induces an average lifespan reduction of 9.83% (2.02 years). Under the extreme compliance limit (constant 105% load, 5% THD), this reduction surges to 22.72% (4.67 years), quantitatively shattering the traditional assumption of "zero damage" in the SCADA green zone. Furthermore, an Equivalent Operating Time (EOT) tracing algorithm based on a 1-year sliding window is proposed to smooth seasonal phase distortions. In exhaustive full-lifecycle traversal tests, this algorithm predicts future extra lifespan losses with an ultra-low average relative error of 0.31% (3.10 days). This framework provides grid dispatchers with computationally lightweight, physically self-consistent indicators for proactive asset management.

Index Terms—Power transformers, total harmonic distortion (THD), sub-threshold harmonics, thermal degradation, hidden lifespan loss, SCADA green zone, IEEE Std C57.110, IEEE Std C57.91.

I. Introduction

In modern transmission and distribution grids, the rapid proliferation of high-penetration inverter-based resources (IBRs), nonlinear industrial drives, and power electronic interfaces has fundamentally altered the power quality characteristics of the grid [1], [2]. Although large-amplitude transient voltage spikes and severe overloads are effectively intercepted by automatic protection devices and relay alarms, the sub-threshold synergistic stresses within the SCADA green zone—namely, continuous minor harmonics operating within standard safety limits (THD $\leq$ 5%, per IEEE Std 519 [2]) and permissible periodic minor overloads (load factor $K \leq 105\%$, per IEC 60076-7 [3])—exist covertly for extended periods and completely fail to trigger static SCADA alarm thresholds.

According to the general equipment specifications in IEEE Std C57.12.00 [4], for 110kV heavy-duty oil-immersed power transformers, sub-threshold harmonic currents induce additional parasitic eddy current losses within large-cross-section copper windings. According to IEEE Std C57.110 [5], winding eddy current losses are proportional to the square of the harmonic order (h^2). Because the ratio of winding eddy current loss to rated I^2R loss for 110kV transformers ($K_{EC} \approx 0.40$) is significantly higher than that for small distribution transformers ($K_{EC} \approx 0.05 \sim 0.15$) [5], even minor harmonic levels can considerably elevate the winding hottest-spot temperature (HST). Under the nonlinear exponential effect stipulated by IEEE Std C57.91, the elevated HST accelerates the thermal degradation of cellulose insulation paper, leading to a covert decline in its degree of polymerization and resulting in the silent degradation of the physical design life [6].

Existing asset health index (HI) evaluations and data-driven remaining useful life (RUL) prediction methods [7], [8] generally place SCADA operational data under a static hard-threshold binary classification: any operational parameters below the alarm limits (e.g., load factor $K \leq 105\%$, distortion rate THD $\leq$ 5%) are uniformly assigned a green "safe" status. Consequently, these models fail to capture the cumulative thermal degradation caused by long-term exposure to sub-threshold stresses. Furthermore, when sensors or monitoring devices are installed midway through the service life of older transformers lacking complete historical SCADA records, traditional RUL algorithms face severe initial condition drift and seasonal phase distortion issues.

To resolve the absolute positioning dilemma and historical ledger dependency of traditional RUL predictions, this paper proposes a dual-engine physics-informed framework for the full-cycle hidden loss quantification and multi-stress decoupling of 110kV heavy-duty oil-immersed power transformers. Based on mature IEEE standard physics, this framework discards guesswork regarding remaining life and systematically characterizes, isolates, and quantitatively calculates the full-lifecycle excess degradation induced by sub-threshold stresses under SCADA-compliant green-zone conditions—revealing a degradation pathway long overlooked in traditional asset management literature.

The main contributions of this paper are summarized as follows:

1) GZDS Scenario Thermal Degradation Quantification Framework (A Dedicated White-Box Quantification

Tool): This paper is the first to formally define the Green-Zone Dual Stress (GZDS) scenario. To the best of the authors' knowledge, this is the first closed-form white-box quantification framework established specifically for this GZDS scenario. By integrating IEEE Std C57.110 and IEEE Std C57.91 into a unified dual-physics engine, this framework constructs a quantitative model that directly maps thermal degradation. 1,000,000 Monte Carlo evolutionary simulations prove that multi-sub-threshold stress synergy causes an average equivalent physical calendar life reduction of 9.83% (based on a 20.55-year baseline life, equivalent to a loss of 2.02 years). Under the extreme condition of a constant 105% load and 5% THD, the equivalent life reduction ratio reaches as high as 22.72% (equivalent to a calendar life loss of 4.67 years), establishing quantitative engineering operational boundaries for proactive life extension.

2) 1-Year Sliding Window Smoothing and Full-Cycle Equivalent Loss Projection: This paper proposes an equivalent projection algorithm based on a 1-year sliding observation window, effectively smoothing the 12-month seasonal thermal cycle errors. In exhaustive traversal tests of continuous monitoring points covering the entire lifecycle, the algorithm achieves an ultra-low average relative error of 0.31% (absolute deviation of 3.10 days) in predicting future remaining extra lifespan losses, demonstrating solid physical self-consistency.

II. Related Work

A. Limitations of Data-Driven Predictions and Ledger Dependency

In recent years, transformer RUL models based purely on data-driven and deep learning approaches have witnessed explosive growth. Numerous studies employ architectures such as Long Short-Term Memory (LSTM) networks, Gated Recurrent Units (GRU), and even large Transformer models [9], [10] to achieve nonlinear fitting of asset degradation trajectories by mining historical SCADA ledgers. Some cutting-edge works also introduce Digital Twin technology [11] or Physics-Informed Neural Networks (PINN) [12] that incorporate physical priors, attempting to reconstruct the health status of transformers in virtual space.

Although these "black-box" algorithms demonstrate extremely high prediction accuracy in temperature-controlled sandbox experiments with massive and continuous historical training data [13], they face fatal limitations in real-world grid operations. Purely data-driven models rely heavily on continuous and complete full-lifecycle ledgers [14]; when sensors are installed midway on older transformers, the lack of historical data (i.e., the existence of long-term historical blind spots) makes the algorithms highly susceptible to initial condition drift. More crucially, these black-box models lack underlying physical causal interpretability and cannot provide grid dispatchers with quantitative intervention indicators that have clear engineering significance, such as "how much load to reduce" or "which harmonic order to suppress."

B. Computational Bottlenecks of White-Box Thermodynamic Modeling

To compensate for the lack of physics in black-box models, another stream of research is dedicated to deepening the white-box thermophysical modeling of transformers. Cutting-edge research introduces Dynamic Thermal Circuit Models [15], [16] and multi-physics coupled Finite Element Analysis (FEA) [13] to meticulously characterize the internal fluid dynamics and heat transfer processes of oil-immersed transformers [1], [6], [15].

Undoubtedly, these models possess impeccable physical rigor. However, whether solving partial differential equation systems or maintaining complex dynamic thermal capacitance networks, extremely high time-domain monitoring frequencies and massive computational power are required [17]. Such "heavy computation" can often only be performed in offline laboratory environments or high-performance computing clusters, and fundamentally cannot be scaled and embedded into modern lightweight grid SCADA dispatch systems, which have extremely limited computational resources and rely on millisecond-level responses. Recently, some studies have utilized order reduction techniques such as Proper Orthogonal Decomposition (POD) to rapidly reconstruct the internal hotspot temperature field of transformers using a small number of sensors [18]. However, when facing complex nonlinear harmonic-load coupling, the boundary consistency and cross-condition generalization capabilities of reduced-order models still face challenges. Therefore, the industry urgently needs a compromise dual-engine framework that strictly adheres to physical laws while remaining extremely lightweight computationally.

C. The Thermal Degradation Blind Spot of Sub-Threshold Harmonics

With the large-scale grid integration of nonlinear loads such as high-penetration IBRs and electric vehicle charging stations, the slight deterioration of power quality has become an unignorable background trend [19], [20]. Extensive research has confirmed that severely excessive high-order harmonics lead to a surge in parasitic eddy currents in transformer windings, thereby causing overheating and even insulation breakdown [21], [22].

However, existing industrial asset management systems still rigidly rely on static hard alarm thresholds. For "compliant sub-threshold harmonics" operating within standard thresholds (e.g., THD $\leq$ 5% per IEEE Std 519), because they do not trigger any limit-exceeding alarms, they are often classified as a "safe green zone" by existing SCADA systems. A few recent cutting-edge studies [23], [24] have begun to alert the industry to the cumulative thermal effects of these long-standing low-amplitude harmonics, but rarely has research unified the temporal decoupling of "minor load fluctuations (100%–105%)" and "sub-threshold harmonics" within the SCADA green zone, nor provided precise quantitative evaluation of the full-cycle hidden lifespan loss caused by their synergy under a white-box physical framework. This synergistic effect, under Arrhenius exponential scaling, further exhibits super-additive penalty characteristics distinct from linear superposition expectations. This is precisely the core engineering gap this framework aims to fill.

Definition 1 (Green-Zone Dual Stress, GZDS): This paper formally defines the synergistic operational state where a transformer simultaneously satisfies $\mathrm{THD}(t) \in [0\%, 5\%]$ (IEEE Std 519 compliance upper limit) and load factor $K(t) \in [100\%, 105\%]$ (periodic load range permitted by IEC 60076-7) as the Green-Zone Dual Stress (GZDS) scenario. The essential characteristic of GZDS is that both types of stress independently reside within their respective standard compliance boundaries, triggering no SCADA alarms; yet, at the physical level, their synergy continuously induces accelerated Arrhenius thermal aging, forming an unignorable hidden lifespan degradation. The dual-engine physics-informed framework proposed in this paper serves as a dedicated white-box quantification tool specifically for the GZDS scenario—whenever a transformer operates within the GZDS state, this framework can be directly applied without any additional preconditions or complex parameter identification.

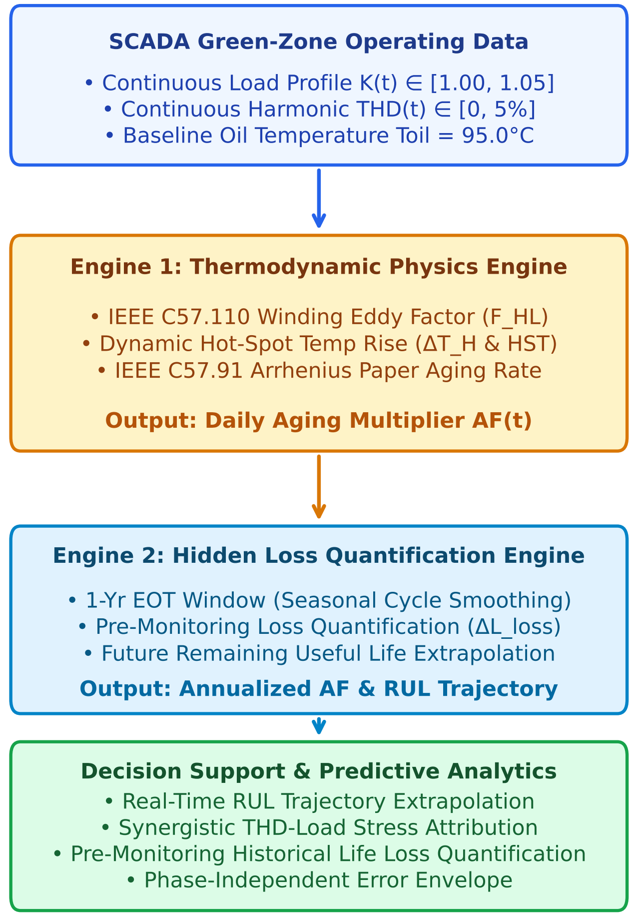

Fig. 1. Overall architecture of the dual-engine physics-informed framework.

III. Methodology and Mathematical Engines

A. Dual-Engine Architecture and Scope

This framework consists of two functionally decoupled white-box engines and a decision-layer output module (Figure 1): the Thermodynamic Engine, the Hidden Loss Quantification Engine, and Decision Support & Predictive Analytics. In terms of thermodynamic modeling, this model primarily quantifies the thermal effects brought by winding parasitic eddy current losses. Although harmonics can also induce non-thermal effects such as increased dielectric losses or partial discharges, these complex microscopic mechanisms are difficult to evaluate accurately using only the macroscopic THD indicator. Therefore, the harmonic thermal aging results evaluated by this model can be regarded as a conservative lower bound of the actual insulation degradation.

1) Thermal Physics Engine: The Thermal Physics Engine is responsible for transforming SCADA operational state parameters (including electromagnetic, power quality, and baseline oil temperature) into thermodynamic damage factors:

- Input Parameters: Dynamic SCADA time-series data (compliant green zone), including top-oil temperature $T_{oil}(t)$, active load factor $K(t)$, and total harmonic distortion $\mathrm{THD}(t)$.
- Embedded Equations: Sequentially executes harmonic loss modification factor $F_{HL}(t)$ via Eq. (1), dynamic winding hottest-spot temperature rise $\Delta T_H(t)$ via Eq. (3), absolute hottest-spot temperature $HST(t)$ via Eq. (4), and Arrhenius thermal aging acceleration factor $AF(t)$ via Eq. (5).
- Core Output: Provides high-granularity (hourly/daily) dynamic lifespan loss acceleration factor $AF(t)$ sequences.

2) Hidden Loss Quantification Engine: The Hidden Loss Quantification Engine is responsible for completing the decoupling of damages and calculating the full-lifecycle excess degradation based on a sliding window:

- Input Parameters: Real-time driven $AF(t)$ acceleration factor time-series generated by the Thermal Physics Engine.
- Embedded Algorithms: Executes the 1-year EOT sliding window average via Eq. (6) to smooth seasonal fluctuations and extract the annualized equivalent acceleration factor ($\overline{AF}_{1yr}$); anchored on the baseline physical lifespan, it maps this factor to the physical time reduction over the full cycle.
- Core Output: Quantitatively outputs the full-cycle hidden loss degree induced by the synergy of load fluctuations (Load) and harmonic distortion (Har-

monics) (i.e., Baseline Life – Baseline Life/$\overline{AF}_{1yr}$ = Excess Loss Years).

3) Decision Support & Predictive Analytics: Based on the cascaded calculation of the dual engines mentioned above, this framework ultimately provides the following decision support at the application layer:

- Full-Cycle Excess Loss Projection: Directly maps the physical reduction of the equipment's overall design life under current conditions based on the 1-year equivalent acceleration factor, avoiding guesswork regarding absolute remaining life.
- THD-Load Synergistic Damage Attribution: Quantitatively decouples the independent and synergistic contributions of load fluctuations and harmonic distortion to the aforementioned full-cycle lifespan reduction.
- Equivalent Historical Baseline Re-evaluation: By projecting short-term high-frequency monitoring loss rates backward, it explicitly fills the hidden loss void caused by the lack of complete historical ledgers prior to sensor installation.
- Phase-Agnostic Smoothing Mechanism: Eliminates short-term thermal stress evaluation error drifts caused by sensors being installed in any arbitrary season (phase) of the year, via a 1-year sliding window.

B. White-Box Mathematical Engine: 4-Step Physical Derivation Chain

1) Step 1: IEEE Std C57.110 Winding Eddy Current Heating Factor: According to IEEE Std C57.110 [5], harmonic currents increase the winding eddy current loss P_{EC}. The winding eddy current heating modification factor $F_{HL}(t)$ is calculated as:

$$F_{HL}(t) = 1 + \sum_{h=2}^{\infty} \left(\frac{I_h(t)}{I_1(t)} \right)^2 \cdot h^2 \approx 1 + h_{eq}^2 \cdot \mathrm{THD}(t)^2 \quad (1)$$

where h_{eq} is the equivalent dominant harmonic order. For 110kV main transformers operating in an environment dominated by 12-pulse rectifiers as nonlinear loads ($h = 12k \pm 1$), $h_{eq} = 12$ is adopted as the arithmetic mean of the 11th and 13th dominant harmonic pairs. (Note: For 6-pulse systems, $h_{eq} = 6$, and F_{HL} is correspondingly lower; $h_{eq} = 12$ represents a typical heavy industrial scenario). To evaluate the robustness of this parameter selection, a sensitivity check for $h_{eq} \in \{11, 12, 13\}$ was conducted: under the green-zone upper limit condition (THD = 5%), when h_{eq} shifts from 12 to 11 or 13, the deviation of F_{HL} is approximately ±4.6%. The impact on the final lifespan loss conclusion is within an engineering acceptable range, demonstrating that the median selection of $h_{eq} = 12$ has sufficient robustness against parameter perturbations.

2) Step 2: Dynamic Winding Hottest-Spot Temperature Rise and Hottest-Spot Temperature (HST): According to the classical load temperature rise theory in IEEE Std C57.91 [6], the active load factor $K(t) = I_{load}(t)/I_{rated}$ is used to correct baseline losses, and the load heating factor $F_{load}(t)$ it induces is formulated as:

$$F_{load}(t) = \left(\frac{K(t)}{K_R} \right)^{2y} \quad (2)$$

where y is the winding hottest-spot temperature rise exponent. Considering that 110kV-class main transformers most commonly adopt ONAN/ONAF (Oil Natural Air Natural / Oil Natural Air Forced) cooling methods, according to the specifications in IEEE Std C57.91 [6], the empirical thermal exponent for such cooling conditions is assigned as $y = 0.8$.

Further combining Eq. (1) and Eq. (2), and adhering to the modification principles recommended by IEEE Std C57.110 [5], the dynamic winding hottest-spot temperature rise $\Delta T_H(t)$ under multi-stress coupling is derived:

$$\Delta T_H(t) = \Delta T_{H,R} \cdot F_{load}(t) \cdot \left[\frac{1 + F_{HL}(t) \cdot K_{EC}}{1 + K_{EC}} \right]^y \quad (3)$$

where $\Delta T_{H,R} = 15.0°\mathrm{C}$ is the rated hot-spot temperature rise gradient for 110kV heavy-duty transformers [6], and $K_{EC} = 0.40$ is the ratio of winding eddy current loss to I^2R loss under rated load [5].

To strictly isolate the independent thermal contributions of load and harmonics at the methodological level, this study adopts the Controlled Variable Approach, fixing the top-oil temperature $T_{oil}(t)$ at its rated steady-state value of 95.0°C. This setup does not deny the dynamic characteristics of oil temperature, but rather eliminates the interference of environmental temperature as an exogenous variable to obtain a deterministic baseline estimate of the independent contributions of THD and load factor to the winding HST. Under this controlled condition, all quantitative conclusions represent a conservative worst-case upper-bound estimate of the thermal aging effects purely induced by the "harmonic + load" synergistic stress (because in real-world scenarios, periods where the oil temperature is lower than the rated steady-state value will decelerate the aging rate, making the true cumulative lifespan loss likely lower than the results estimated by this framework). Thus, the absolute hottest-spot temperature $HST(t)$ is obtained:

$$HST(t) = T_{oil}(t) + \Delta T_H(t) \quad (4)$$

3) Step 3: IEEE Std C57.91 Arrhenius Aging Acceleration Factor: Relative to the reference rated HST_R = 110.0°C (383.15 K, corresponding to $AF = 1.0$ and a baseline insulation life of 180,000 hours / 20.55 years), the real-time insulation paper aging acceleration factor $AF(t)$ is calculated according to the Arrhenius relationship [6]:

$$AF(t) = \exp\left(\frac{B}{383.15} - \frac{B}{HST(t) + 273.15} \right) \quad (5)$$

where $B = 15,000$ K is the activation energy constant for thermally upgraded insulation paper.

To intuitively demonstrate the nonlinear characteristics driven jointly by the "electromagnetic heating layer" (Equation (3)) and the "Arrhenius thermal aging layer"

(Equation (5)) in the dual engines, Figure 2 plots the thermal aging acceleration surface under the synergy of multiple compliant stresses. From the figure, two layers of hidden damage can be clearly observed: first, even within the traditional SCADA green zone, pure load fluctuations and sub-threshold harmonics independently consume a portion of the transformer's lifespan (manifested as an overall baseline elevation of the surface); more fatally, under the joint action of load and harmonics, the two do not merely superimpose linearly but produce a intense multiplicative amplification effect. As both the load factor and harmonics approach the upper limits of the green zone simultaneously, the thermal aging surface exhibits an extremely steep exponential "tailing" phenomenon. This "super-additive" physical penalty is precisely the hidden thermal degradation mechanism easily misjudged by traditional static threshold monitoring and linear superposition methods.

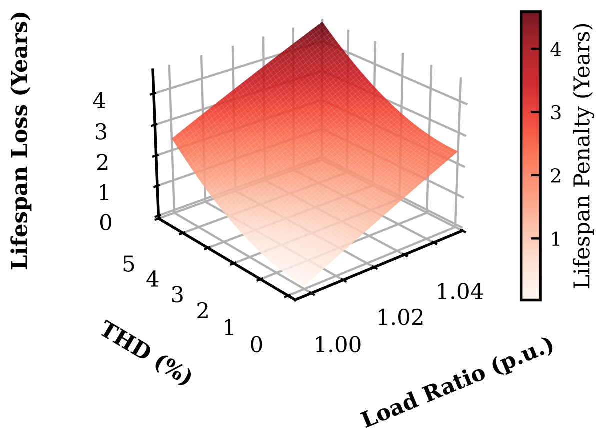

Fig. 2. Thermal aging acceleration surface under the linkage of varying compliant load factors and THD.

4) Step 4: 1-Year Sliding Window-Based Full-Cycle Equivalent Loss Evaluation Method: To decouple the interferences of environmental temperature and local seasonal fluctuations, and strictly isolate the true thermal fatigue loss driven by THD and active load, this paper proposes a full-lifecycle physical loss equivalent projection algorithm based on a 1-year sliding window, under the assumption of macro-stationarity of the transformer's historical load profiles. First, the model calculates the equivalent annualized aging acceleration factor $\overline{AF}_{1yr}(t_{now})$:

$$\overline{AF}_{1yr}(t_{now}) = \frac{1}{365} \sum_{j=t_{now}-365}^{t_{now}} AF(t_j) \tag{6}$$

This 365-day window covers a complete annual cycle of grid load and environmental temperature, physically smoothing out seasonal phase deviations.

To achieve a universal evaluation independent of the equipment's initial state and absolute design lifespan, a dimensionless indicator is extracted—the full-cycle equivalent excess aging rate (i.e., physical calendar lifespan reduction ratio) $\Delta L_{\%}$:

$$\Delta L_{\%}(t_{now}) = 1 - \frac{1}{\overline{AF}_{1yr}(t_{now})} \tag{7}$$

This indicator represents the relative proportion by which the transformer's lifecycle is prematurely overdrawn under current multi-stress boundaries. For a specific transformer, its actual physical calendar lifespan reduction amount ΔL_{loss} can be directly calculated by incorporating its rated design lifespan L_{rated}:

$$\Delta L_{loss}(t_{now}) = L_{rated} \cdot \Delta L_{\%}(t_{now}) \tag{8}$$

Furthermore, to provide frontline grid dispatchers with the most actionable indicator, this framework discards tracing already occurred sunk costs and shifts the evaluation focus to "future penalties." First, based on the physical calendar time the transformer has already served (T_{used}), the historically consumed equivalent standard lifespan $L_{consumed}$ is calculated:

$$L_{consumed}(t_{now}) = T_{used} \cdot \overline{AF}_{1yr}(t_{now}) \tag{9}$$

Subsequently, decision-makers can directly solve for the hidden additional reduction of future remaining lifespan (ΔL_{future_loss}):

$$\begin{aligned}\Delta L_{future\_loss}(t_{now}) =& (L_{rated} - L_{consumed}(t_{now})) \\ & \cdot \Delta L_{\%}(t_{now})\end{aligned} \tag{10}$$

This ΔL_{future_loss} indicator translates the abstract thermophysical aging multiplier into the expected extra reduction (in days or years) of the transformer's future physical calendar lifespan under current harmonic distortion and load levels. Its core engineering purpose is to directly expose the hidden accelerated degradation effect of THD and minor overloads within the SCADA green zone on the full lifecycle of the transformer, providing a direct quantitative decision-making basis for maintenance personnel to take early intervention measures (e.g., installing active power filters, load peak-shaving and valley-filling).

IV. Experiments and Results

A. Numerical Simulation Setup and Green-Zone Boundaries

A sandbox environment is constructed for a 110kV heavy-duty oil-immersed power transformer. The baseline design life strictly follows the IEEE Std C57.91 threshold of 180,000 hours (equivalent to 20.55 years or approximately 7,500 days) of continuous operation at a 110°C winding hottest-spot temperature [6]. The lower bound for the load factor is set to $K = 100\%$ (rated full load) rather than a lower condition: according to IEEE Std C57.110 [5], the nonlinear amplification effect of the eddy current loss factor K_{EC} on the hot-spot temperature rise is most pronounced at or near rated load; under underload conditions ($K < 100\%$), the marginal thermal degradation effect of the GZDS dual-stress synergy is relatively limited and falls outside the specific application boundaries defined

TABLE I
Numerical Simulation Boundaries Under SCADA Green-Zone Compliance Constraints

Parameter / Constraint	Standard Boundary	Physical Meaning / Source
Top-Oil Temp (T_{oil})	Constant 95.0°C	Rated steady state [6]
Rated HST Rise ($\Delta T_{H,R}$)	15.0°C	110kV heavy-duty [6]
Active Load Factor (K)	Uniform $[1.00, 1.05]$	IEC 60076-7 cyclic overload [3]
Harmonic THD	Uniform $[0.00, 0.05]$	IEEE 519 safety green zone [2]
Eddy Loss Ratio (K_{EC})	0.40	110kV heavy-duty [5]
Eq. Harmonic Order (h_{eq})	12.0	12-pulse dominant [5]
Baseline Life (L_{rated})	20.55 yrs (180k h)	Insulation baseline [6]

by this framework. All other core parameter boundaries of the sandbox are constrained by SCADA green-zone compliance criteria (with uniform distributions representing a conservative neutral assumption of equiprobable occurrence of compliant stresses), as detailed in Table I. The subsequent population degradation distribution evaluations (Section IV-B) and EOT algorithm prediction accuracy tests (Section IV-C) strictly employ multiple Monte Carlo random sampling and time-series simulations within the compliant boundaries defined in Table I.

B. RUL Trajectory Drill and Quantitative Attribution Decoupling

To ensure the statistical convergence of random sampling within the multi-dimensional parameter space, this study executed 1,000,000 independent Monte Carlo trials within the established green-zone sandbox boundaries. The comprehensive statistical indicators and quantitative comparisons against three baseline scenarios (namely: Scenario 1 Nominal Baseline, Scenario 2a Pure Load Stress, and Scenario 2b Pure Harmonic Stress) are shown in Table II:

Under compliant SCADA green-zone operation (Scenario 3), the actual average lifespan of transformers sampled across 1,000,000 Monte Carlo trials drops to 18.53 years, equivalent to a mean lifespan degradation of 9.83% (2.02 years / 737 days) compared to the nominal 20.55-year lifespan, as illustrated in Table II and Figure 3(a). It is noteworthy that the probability density histogram in Figure 3(a) further completely outlines the physical envelope of lifespan decay (based on the statistical results of the 1,000,000 samples, with a distribution standard deviation $\sigma \approx 0.97$ years). Although the input load factor (100% $\sim$ 105%) and THD (0% $\sim$ 5%) are set to uniform distributions within the green zone, due to the nonlinear superposition of the hot-spot temperature and the exponential scaling effect of the Arrhenius aging rate, the ultimately mapped physical lifespan presents an asymmetric, wide-band envelope distribution. This envelope boundary (the lower limit approaches the worst-case extreme of 15.88 years, while the upper limit is close to the baseline of 20.55 years) intuitively reveals that: even fully within the SCADA alarm blind spot (green zone), the combination of multiple minor stresses under different operational conditions can still lead to immense lifespan uncertainty. This proves that relying solely on single-parameter static green zones fails to reflect true population asset risks. It must be emphasized that the aforementioned 9.83% and 22.72% quantitative loss conclusions are specific profiles derived based on the typical $K_{EC} = 0.40$ of 110kV heavy-duty transformers; for distribution-level transformers with smaller K_{EC} values, the degradation ratio will scale accordingly, which serves as an intuitive demonstration of the cross-capacity evaluation generalization capability of this quantitative framework.

To clearly demonstrate the joint degradation effect under multiple stresses, Figure 3(b) and Table III provide a super-additive breakdown of the quantitative indicators under the green-zone upper limit (Scenario 4). The waterfall chart intuitively separates the pure load loss, pure harmonic loss, and the additional lifespan loss caused by their nonlinear coupling; while the table strictly traces the formulas back to the physical derivation steps in Section III of this paper.

As shown in Table III, due to the nonlinear characteristics of the Arrhenius exponential equation, the true combined aging acceleration factor (1.294) is strictly greater than the linear simple addition expectation (1.262). This super-additive penalty is ultimately amplified into an absolute extra lifespan loss of 0.40 years through the engineering expansion equation (??). This proves that when evaluating the SCADA green-zone status of transformers, the traditional independent linear superposition rule will severely underestimate the true physical thermal degradation.

C. EOT Sliding Window Prediction Accuracy and Error Convergence

To verify the accuracy and robustness of the EOT sliding window algorithm in Step 4 for quantitatively evaluating future remaining extra lifespan losses, this study simulated a complete transformer lifecycle trajectory superimposed with a 1-year cyclic "dual-peak summer/winter" sinusoidal profile and high-frequency random noise. Continuous traversal tests were performed on this trajectory (i.e., t_{inst} incrementally stepping daily from day 0 up to a cutoff of $T_{fail} - 365$ days).

As shown in Figure 4, the 1-year EOT tracing algorithm effectively smooths out high-frequency random fluctuation interferences from local loads and harmonics. The continuous exhaustive evaluation of the entire transformer lifecycle (covering all valid potential sensor access points within $t_{inst} \in [0, T_{fail} - 365$ days$]$) indicates that the overall average relative error in predicting future remaining

TABLE II
Quantitative Comparison of Lifespan Indicators for Typical Operating Scenarios Under 1,000,000 Monte Carlo Trials

Operating Scenario	THD Range	Load Range	Avg. HST (°C)	Avg. Aging Rate ($\overline{AF}$)	Avg. Actual Life (Yrs)	Life Loss
Scenario 1: Nominal Baseline	0.0%	100.0%	110.00	1.000	20.55 yrs (7500.0 d)	0.00% (0.00 yrs)
Scenario 2a: Pure Load Stress	0.0%	100% ∼ 105%	112.51	1.064	19.31 yrs (7046.7 d)	6.03% (1.24 yrs)
Scenario 2b: Pure Harmonic	0% ∼ 5%	100.0%	110.41	1.043	19.70 yrs (7190.5 d)	4.12% (0.85 yrs)
Scenario 3: Joint Green Zone	0% ∼ 5%	100% ∼ 105%	114.42	1.112	18.53 yrs (6763.5 d)	9.83% (2.02 yrs)
Scenario 4: Green-Zone Limit	5.0%	105.0%	118.84	1.294	15.88 yrs (5796.0 d)	22.72% (4.67 yrs)

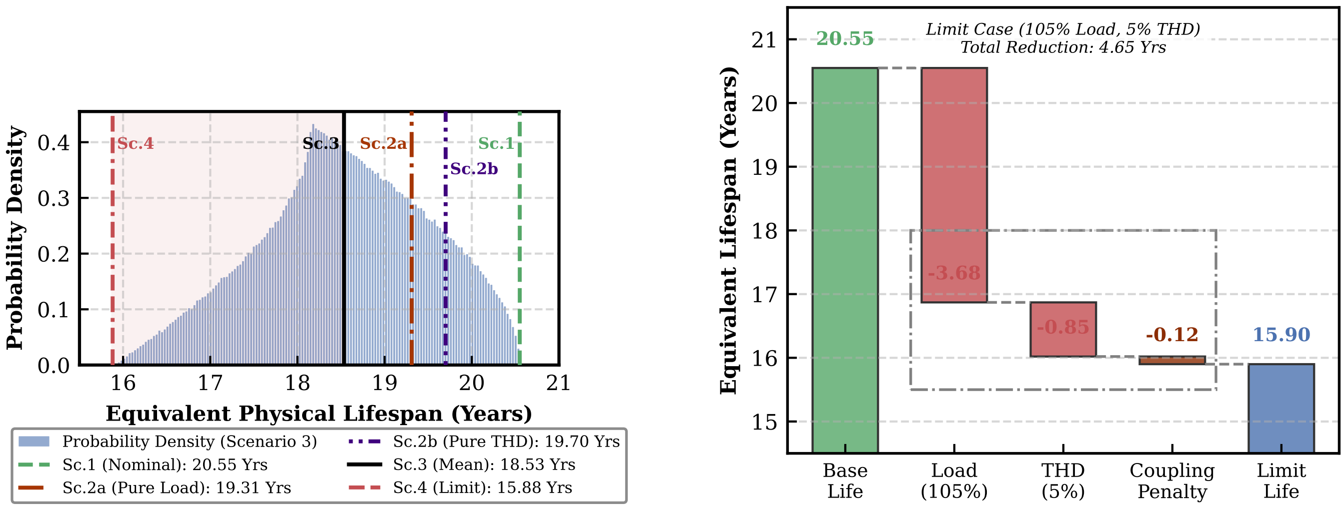

(a) Equivalent lifespan probability distribution from Monte Carlo evolution (Macro-result)

(b) Hidden lifespan loss decoupling and attribution under extreme condition (Micro-attribution)

Fig. 3. Full-cycle lifespan evaluation and thermal aging decoupling under multiple sub-threshold stresses. (a) Equivalent lifespan probability distribution; (b) Hidden lifespan loss decoupling waterfall chart.

TABLE III
Multi-Stress Quantitative Decoupling, Formula Traceability, and Super-Additive Effect Analysis (Taking Scenario 4 Extreme Condition as an Example)

Analysis Dimension	Key Evaluation Metric	Result	Traceability	Physical Meaning / Conclusion
Independent Stress	Pure Load AF (AF_{load} @ 105% load, 0% THD)	1.131	Step 3, Eq. (5)	Independent aging rate from extreme minor overload
	Pure Harmonic AF (AF_{THD} @ 100% load, 5% THD)	1.131	Step 3, Eq. (5)	Independent aging rate from extreme sub-threshold harmonics
Super-Additive	Linear Expected AF (AF_{linear} @ 105% load, 5% THD)	1.262	Simple addition ($AF_{load}+AF_{THD}-1$)	Theoretical expectation assuming no nonlinear coupling
	True Combined AF ($AF_{combined}$ @ 105% load, 5% THD)	1.294	Step 2, Eq. (3)	True extremum induced by strong multiplicative coupling of F_{load} and F_{HL}
	Extra Super-Additive Penalty	+0.032	True minus expected	"1+1>2" penalty amplified by Arrhenius exponential equation
Lifespan Reduction	Extra Lifespan Loss (Super-Additive)	0.40 yrs	Step 4, Eq. (??)	Absolute calendar lifespan reduction caused by super-additive penalty

extra lifespan loss (ΔL_{future_loss}) is a mere 0.31% (an average absolute deviation of 3.10 days). The extremely narrow continuous error envelope confirms that this framework possesses exceptionally high internal physical self-consistency and immunity to operational fluctuations under the premise of stationary conditions.

V. Conclusion and Future Work

All quantitative conclusions in this study are fundamentally established upon a rigorous baseline premise: according to IEEE Std C57.91, the physical design life of a transformer operating continuously at a 110°C winding

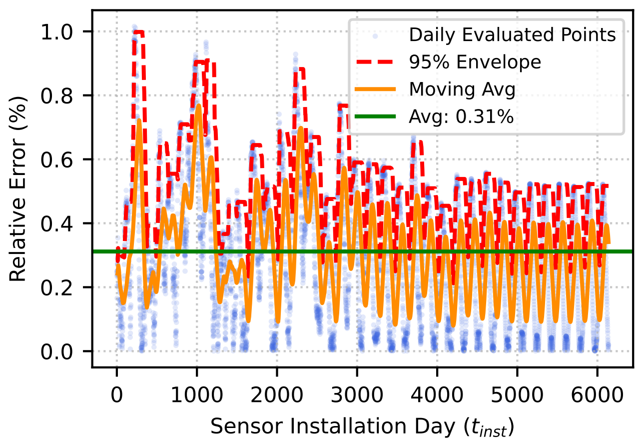

Fig. 4. Internal self-consistency verification of the EOT algorithm: Relative error rate and convergence envelope for future remaining extra lifespan loss prediction (average relative error: 0.31%, average absolute deviation: 3.10 days) through an exhaustive full-lifecycle traversal (5,906 continuous intermediate sampling points) within the physically consistent framework assuming macroscopic stationarity.

hottest-spot temperature is 180,000 hours (equivalent to 20.55 years, or approximately 7,500 days). Based on this premise, this paper proposes a white-box dual-engine physics-informed framework for quantifying hidden thermal degradation and extra lifespan loss for 110kV power transformers under the GZDS scenario. The applicability trigger conditions for this framework are explicit and lightweight: Whenever a transformer's operational state satisfies THD $\in [0\%, 5\%]$ and $K \in [100\%, 105\%]$, it enters the GZDS scenario, and this framework can be directly invoked. This implies that any 110kV main transformer operating near full load with background harmonics in modern power grids must incorporate this framework into its health evaluation system. By integrating IEEE Std C57.110 and C57.91, this framework successfully resolves a critical SCADA monitoring blind spot:

1) The synergistic fluctuation of compliant sub-threshold harmonics (0%–5% THD) and minor overloads (100%–105%) induces an average baseline lifespan loss of up to 9.83% (2.02 years). Under the extreme scenario of constant 105% load and 5% THD, the loss ratio surges to 22.72% (4.67 years), establishing a quantitative operational window of $[0, 4.67$ years$]$ and shattering the traditional assumption of "zero damage" in the green zone.
2) The 1-year EOT tracing algorithm perfectly smooths the 12-month seasonal phase distortions. In continuous monitoring point traversal tests covering the full lifecycle without blind spots, it achieves an ultra-low predictive average relative error of 0.31% (3.10 days).

Limitations and Future Work will focus on: (i) Tracing errors and mitigation strategies under non-stationary conditions: The framework's current exceptionally low prediction error relies on the assumption of annual macroscopic stationarity in load characteristics. If the equipment's historical operational conditions experienced severe non-linear abrupt changes (e.g., massive plant expansions), tracing backward using a single-year window will yield inherent errors. To avoid such errors, the engineering rule of thumb is: the earlier data collectors are deployed and the higher the full-lifecycle data coverage, the smaller the tracing error will be; (ii) Developing a reverse operation and maintenance prescription tool based on this framework to back-calculate the hottest-spot temperature upper limit given a target life extension, thereby outputting actionable synergistic control limits for THD and load for the industry; (iii) Expanding the thermodynamic engine to dynamic ambient temperature profiles and dynamic thermal time constants; (iv) Extending the application to distribution-class transformers ($K_{EC} \approx 0.05 \sim 0.15$) and dry-type transformers; (v) Conducting field validations using authentic multi-year SCADA operational records from grid companies.

References

[1] A. Abeysekara, C. Ekanayake, H. Ma, and T. K. Saha, "Investigation of inverter transformer thermal modelling under supra-harmonics and wind dynamics," IEEE Trans. Power Del., doi: 10.1109/TPWRD.2026.3707912, 2026.

[2] IEEE Standard for Harmonic Control in Electric Power Systems, IEEE Std 519-2022 (Revision of IEEE Std 519-2014), pp. 1–31, 5 Aug. 2022, doi: 10.1109/IEEESTD.2022.9848440.

[3] Power Transformers – Part 7: Loading Guide for Mineral-Oil-Immersed Power Transformers, IEC Standard 60076-7:2018, 2018.

[4] IEEE Standard for General Requirements for Liquid-Immersed Distribution, Power, and Regulating Transformers, IEEE Std C57.12.00-2021, 2021.

[5] IEEE Recommended Practice for Establishing Liquid-Immersed and Dry-Type Power and Distribution Transformer Capability When Supplying Nonsinusoidal Load Currents, IEEE Std C57.110-2018, 2018.

[6] IEEE Guide for Loading Mineral-Oil-Immersed Transformers and Step-Voltage Regulators, IEEE Std C57.91-2011, 2012.

[7] A. El Maghraoui, O. Laayati, H. El Hadraoui, Y. Ledmaoui, and A. Chebak, "AI-driven proactive maintenance scheduling for power transformers using physics-informed deep learning and economic optimization," in Proc. 2026 8th Global Power, Energy Commun. Conf. (GPECOM), 2026, pp. 268–274, doi: 10.1109/GPECOM70462.2026.11578752.

[8] S. N. Prakash, S. G. Nandan, A. A. K. Chaudhury, S. Yomesh, and J. Hari, "Cost reduction of distribution transformers using IoT-enabled predictive health index and remaining useful life estimation with machine learning," in Proc. 2026 Int. Conf. Innov. Emerg. Technol. Sustain. Dev. (ICIETSD), 2026, pp. 1–5, doi: 10.1109/ICIETSD68684.2026.11584861.

[9] Z. Xing and Y. He, "Improved neural controlled differential equation for remaining useful life prediction of power transformers," in Proc. 2023 Prognostics Health Manage. Conf. (PHM), 2023, pp. 29–33, doi: 10.1109/PHM58589.2023.00014.

[10] G. A. Ginja, A. A. A. de Queiroz, and J. P. P. do Carmo, "Physics-informed prognostic assessment of transformer oil aging via ultrasonic sensing and an integro-difference framework," IEEE Trans. Instrum. Meas., vol. 75, pp. 9527507, 2026, doi: 10.1109/TIM.2026.3704259.

[11] L. A. Burnett, U. M. Nabila, and M. I. Radaideh, "Variational digital twins," Energy AI, vol. 24, May 2026, Art. no. 100756, doi: 10.1016/j.egyai.2026.100756.

[12] J. Liang, J. Fan, G. Zhang, and W. D. Van Driel, "A multi-agent system for automated lifetime prediction of power electronics," in Proc. 2026 27th Int. Conf. Therm. Mech. Multi-Physics Simul. Exp. Microelectron. Microsyst. (EuroSimE), 2026, pp. 1–6, doi: 10.1109/EuroSimE69483.2026.11511926.

[13] J. Zhang, M. Jian, H. Zhu, and L. Yang, “A remaining useful life prediction framework for IGBT based on dynamic precursor weighting,” IEEE Trans. Power Electron., vol. 41, no. 9, pp. 16129–16143, 2026, doi: 10.1109/TPEL.2026.3680653.

[14] K. Oueslati, N. Dhahbi-Megriche, F. Bragone, K. Morozovska, T. Laneryd, and M. Luvisotto, “Physics-informed neural networks for modelling insulation paper degradation in power transformers,” in Proc. 2022 IEEE Int. Conf. Elect. Sci. Technol. Maghreb (CISTEM), vol. 4, 2022, pp. 1–6, doi: 10.1109/CISTEM55808.2022.10043884.

[15] D. Susa, M. Lehtonen, and H. Nordman, “Dynamic thermal modelling of power transformers,” IEEE Trans. Power Del., vol. 20, no. 1, pp. 197–204, 2005, doi: 10.1109/TPWRD.2004.835255.

[16] D. Susa and M. Lehtonen, “Dynamic thermal modeling of power transformers: further Development-part II,” IEEE Trans. Power Del., vol. 21, no. 4, pp. 1971–1980, 2006, doi: 10.1109/TPWRD.2005.864068.

[17] A. Hamadi, S. Afshar, M. S. Alam, and S. A. Arefifar, “Power transformer harmonic and electro-thermal modeling: a multiphysics review,” IEEE Access, vol. 14, pp. 58590–58618, 2026, doi: 10.1109/ACCESS.2026.3683994.

[18] H. Wang, Z. Wang, D. Xia, and C. Huang, “Power transformer hot-spot temperature inversion based on Gappy-POD,” in Proc. 2024 4th Int. Conf. Smart Grid Energy Internet (SGEI), 2024, pp. 464–467, doi: 10.1109/SGEI63936.2024.10914317.

[19] D. Braga, “Power quality considering the massive integration of variable renewable energy sources,” in Proc. 2023 Int. Conf. Electromech. Energy Syst. (SIELMEN), 2023, pp. 1–6, doi: 10.1109/SIELMEN59038.2023.10290824.

[20] H. M. Usman, R. ElShatshat, and A. H. El-Hag, “Distribution transformer remaining useful life estimation considering electric vehicle penetration,” IEEE Trans. Power Del., vol. 38, no. 5, pp. 3130–3141, 2023, doi: 10.1109/TPWRD.2023.3265671.

[21] Y. Li et al., “The influence of harmonics on the loss and temperature distribution characteristics of converter transformers,” in Proc. 2024 3rd Int. Conf. Energy Elect. Power Syst. (ICEEPS), 2024, pp. 1047–1052, doi: 10.1109/ICEEPS62542.2024.10693087.

[22] Sumaryadi, B. Cahyono, and I. Arifianto, “Diagnostic degradation process of power transformer insulation system: Harmonic current impact to capability of transformer #7 Pulogadung s/s,” in Proc. 2009 IEEE 9th Int. Conf. Prop. Appl. Dielectr. Mater., 2009, pp. 216–219, doi: 10.1109/ICPADM.2009.5252467.

[23] A. Elmoudi, M. Lehtonen, and H. Nordman, “Effect of harmonics on transformers loss of life,” in Conf. Rec. 2006 IEEE Int. Symp. Electr. Insul., 2006, pp. 408–411, doi: 10.1109/ELINSL.2006.1665344.

[24] S. Thakur, N. M. Butlero, and J. Holbøll, “Effects of harmonics on temperature rise and power loss of a distribution transformer,” in Proc. 2022 9th Int. Conf. Condition Monitoring and Diagnosis (CMD), 2022, pp. 732–735, doi: 10.23919/CMD54214.2022.9991585.